Fermi National Accelerator Laboratory

FERMILAB-Pub-94/025-E

E683

Observation of Jet Production by Real Photons

D. Adams et al
The E683 Collaboration

Fermi National Accelerator Laboratory
P.O. Box 500, Batavia, Illinois 60510

January 1994

Submitted to *Physical Review Letters*

Operated by Universities Research Association Inc. under Contract No. DE-AC02-76CHO3000 with the United States Department of Energy

Disclaimer

Observation of Jet Production by Real Photons

E683 COLLABORATION

D. Adams[6], S. Ahmad[6],N. Akchurin[3], P. Birmingham[7], H. Breuer[4], C. C. Chang[4], S. Cihangir[2], M. D. Corcoran[6], W. L. Davis[1], H. R. Gustafson[5], H. Holmgren[4], P. Kasper[2], J. Kruk[6], D. Lincoln [6], M. J. Longo[5], J. Marraffino[2], J. McPherson[3], H. E. Miettinen[6], G. Morrow[6], G. S. Mutchler[6], D. Naples[4,a], Y. Onel[3], J. Skeens[6], G. P. Thomas[1], M. M. Traynor[6], J. W. Waters[7], M. S. Webster[7], J. P. Xu[6], Q. Zhu[6,b]

[1] *Ball State University, Muncie, IN 47306*
[2] *Fermilab, Batavia, IL 60510*
[3] *University of Iowa, Iowa City, IA 52242*
[4] *University of Maryland, College Park, MD 20742*
[5] *University of Michigan, Ann Arbor, MI 48109*
[6] *Rice University, Houston, TX 77005*
[7] *Vanderbilt University, Nashville, TN 37235*
[a] *Present address, Fermilab, Batavia, IL 60510*
[b] *Present address, University of California, Riverside, CA 92521*

Abstract

Interactions of high energy photons on a hydrogen target have been studied using a large acceptance segmented calorimeter. The event topology clearly shows the production of dijet final states as predicted by perturbative QCD. The energy flow in the photon (forward) direction is compared both to Monte Carlo expectations and to that produced in πp interactions.

PACS numbers: 13.60.Hb, 13.87.Ce

Jets arise from the fragmentation of partons in hard scattering processes. Jets have been observed in many experiments in hadron-hadron interactions [1] as well as in deep inelastic lepton-hadron interactions [2] and e^+e^- annihilations [3]. Single high p_t hadrons and energy flow distributions have been studied in earlier, lower energy, photoproduction experiments [4], but until now no observation has been made of jet production by a real photon beam. Recent results from HERA show evidence for hard scattering in quasi-real photon-proton interactions[5]. In this letter we report the first observation of jets produced by a real photon beam incident on a proton target.

In low momentum-transfer processes, photon interactions leading to hadronic final states can be described by the vector-dominance model (VDM), in which photons act like vector mesons [6]. But at high momentum transfer (high p_t), other processes are expected to dominate [7]. These include the direct coupling contribution, in which the photon couples directly into the hard scattering process, and the so-called "resolved" or "anomalous" photon contributions, in which the photon first dissociates into a quark-antiquark pair before interacting. In the direct coupling process, the photon completely disappears, leaving no spectator remnant. The final state consists of three jets: two high-p_t jets and a soft target jet. In both the VDM and "resolved" contributions, the photon has a spectator remnant, thus producing a four-jet final state. In the p_t range of this experiment, VDM processes are not expected to contribute appreciably, while the direct and resolved contributions are expected to compete [8]. When higher-order QCD diagrams are considered, there is no sharp distinction between the direct and resolved processes, but with well-defined experimental cuts, it might be possible to divide events into categories which approximate the Born-level contributions, and quantitative comparisons between data and theory can then be made.

We have observed the photoproduction of high p_t jets in experiment E683 in the Wide Band photon beam at Fermilab which is the world's highest energy tagged photon

beam. Jets have been observed with single jet p_t's in the range 3 GeV/c to 9 GeV/c. Incident tagged photon energies ranged from 50 to 400 GeV. Photons were produced by bremsstrahlung from a secondary electron beam incident on a lead radiator which was 20% of a radiation length. The incoming electron beam had a mean momentum of 310 GeV/c and an rms momentum spread of $\pm 15\%$. The energy of the incoming electrons was tagged by an array of silicon microstrip detectors upstream, between, and downstream of a pair of dipole magnets. Two planes of scintillation counters near the silicon detectors monitored beam flux and occupancy of nearby beam buckets. After the electron radiated, sweeper magnets bent it into an array of shower counters which measured the electron's final energy. The photon energy (excluding effects of multiple bremsstrahlung) is the difference between the incoming and outgoing electron energies, and is known to $\pm 2\%$. Monte Carlo simulations of the beam indicate that our trigger selects against events in which significant multiple bremsstrahlung occurred, so that such effects lead to less than a 5% overestimate of the photon energy. We have not corrected for this effect.

The experimental apparatus is shown in Figure 1. Two scintillation counters upstream of the hydrogen target vetoed charged particles from photons which had converted in material upstream. A counter immediately downstream of the target required at least one charged particle exiting the target. Two planes of scintillator hodoscopes vetoed events which were accompanied by an off-axis muon. Downstream of the target were five planes of multiwire proportional chambers and six planes of drift chambers, followed by an analysis magnet and an additional 13 planes of drift chambers. The magnet had a small p_t kick (about 100 MeV/c) so as not to interfere with calorimeter-based jetfinding.

Following the wire chambers was a highly segmented electromagnetic and hadronic main calorimeter (MCAL), covering a laboratory pseudorapidity (η) range from 2.6 to 4.9, corresponding to laboratory polar angles (θ_L) of 0.8 ° to 8.5 °. The MCAL has been described in detail elsewhere [9]. It consisted of 132 towers of lead-scintillator and steel-

scintillator sampling calorimetry, each tower being four layers deep. Each tower covered a $\Delta\eta$ and azimuthal ($\Delta\phi$) range of about 0.3. Measured energy resolutions were $\frac{\sigma}{E} = \frac{35\%}{\sqrt{E}}$ for electromagnetic particles and $\frac{85\%}{\sqrt{E}}$ for hadrons, where E is in GeV. The absolute energy scale of the calorimeter in this analysis is uncertain to about 7%.

A beam calorimeter (BCAL) downstream of the main calorimeter measured the energy flow in the forward direction, completely overlapping MCAL, so that there were no gaps in forward direction. BCAL covered a θ_L range of 0° to 1.3 °. The BCAL was divided into four layers longitudinally, all of which were steel-scintillator sampling calorimetry. Electromagnetic showers were contained mostly in the first layer, with a small spillover into the second layer. The pattern of longitudinal energy deposition allowed an approximate separation of electromagnetic and hadronic contributions. The energy resolutions were about $\frac{45\%}{\sqrt{E}}$ for electromagnetic particles and $\frac{75\%}{\sqrt{E}}$ for hadronic particles.

The high transverse energy (E_t) trigger was formed using information from MCAL. Analog signals from the four layers in a tower were added, then weighted by $sin\theta_L$ to make signals proportional to E_t for each tower. These signals were then used to form various triggers. For this analysis two trigger types were used, the total E_t or "global" trigger, and the "two-high" trigger. The global trigger required the total E_t in the calorimeter to be above a threshold; this trigger reached full efficiency at a total calorimeter E_t of typically 8 GeV. The two-high trigger required the E_t in any two towers anywhere in the calorimeter to be above a threshold which, for full efficiency, was typically 0.75 GeV. A software threshold slightly above the hardware thresholds removed any biases due to the hardware trigger. The trigger requirement resulted in an effective photon spectrum ranging from about 100 GeV to 400 GeV with a mean of 260 GeV.

A total of four million triggers from the hydrogen target were collected. A small amount of data (about 10% of the photon sample) was collected using a pion beam of mean momentum 250 GeV/c. Data were collected from July 1991 to January 1992. The

data presented here represent about 30% of the photon sample and all of the pion sample. Cuts were applied to remove spurious muon triggers, which were about 12% of the triggers. All events were required to have a reconstructable photon energy. In this analysis no information from the wire chambers has been used. Target empty subtractions of about 20% have been applied to all distributions.

A standard jet-finding algorithm [10] was applied to the MCAL information in the laboratory frame. A cone in pseudorapidity (η) and azimuthal angle (ϕ) was defined by $R = \sqrt{\Delta\eta^2 + \Delta\phi^2}$. The highest p_t tower in an event was used as a seed to define the zero of $\Delta\eta$ and $\Delta\phi$. A cone of radius R=1 was used to define a jet centered around this tower. All towers which fell into this cone were defined to be part of the jet and were used to determine a new jet axis by an energy-weighted sum. The new jet axis was used to define a new cone, and the process was iterated until the jet p_t converged. The procedure was then repeated to search for additional jets, excluding any towers used in the first jet. Results are presented below for events in which the jetfinder located at least two jets, with the average p_t of the two hottest jets at least 4 GeV/c. A fiducial cut of 2° to 6° in θ_L has been made on the reconstructed jet axes to ensure jet containment in the calorimeter. In this θ_L region, the calorimeter had full azimuthal acceptance. The average jet p_t spectrum above p_t of 4 GeV/c was identical for the two triggers, and we make no distinction as to trigger type.

Evidence for jet production can be seen in a number of distributions. Figure 2(a) shows an E_t flow distribution for γp interactions. In this plot the higher p_t jet defines $\phi = 0°$. Each calorimeter tower is plotted at the appropriate ϕ from this axis, with the entry being weighted by the tower E_t. The "trigger" jet, near $\phi = 0$ and the "away-side" jet, near $\phi = 180°$ are apparent. The opposite-side jet appears to be broader than the higher p_t jet, but in fact this apparent widening is due to the departure of the azimuthal opening angle between the jets ($\Delta\phi_{jj}$) from 180° event by event. A similar effect has been

observed in jets produced in $p\bar{p}$ interactions [11]. Figure 2(b) shows $\Delta\phi_{jj}$. The coplanar structure of the events is clear evidence for dijet production.

The data are compared to Monte Carlo events generated using TWISTER V1.2, which generates resolved photons and VDM processes, and LUCIFER V2.2, which generates the direct coupling processes [13]. These calculations are to leading order only, and the direct, resolved, and VDM processes are considered distinct. For the resolved processes, the photon structure function used is that of Duke and Owens [12]. Several proton structure functions are available in the program, but we are insensitive to this choice. The results shown are using EHLQ set 1 [14], with the standard first-order definition of α_s and $\Lambda_{QCD} = 0.2$ GeV. The Q^2 definition used is $Q^2 = \frac{\hat{s}\hat{t}\hat{u}}{\hat{s}^2+\hat{t}^2+\hat{u}^2}$ where $\hat{s}$, $\hat{t}$ and $\hat{u}$ are the Mandelstam variables at the parton level. A minimum p_t of the hard scatter ($\hat{p}_t$) of 2 GeV/c has been used, and for events which pass the jet p_t cuts, the results are not sensitive to this cutoff. The energy spread of the beam has been simulated by generating Monte Carlo events at six different energies, in ratios appropriate to reproduce the observed photon energy spectrum. We have used both the independent fragmentation (IF) option [15] and the string fragmentation (SF) option [16] in the Monte Carlo calculation. Agreement between the Monte Carlo simulation and the data is quite reasonable, as shown in Figure 2, with the IF option giving a slightly better representation of the data. The SF option underestimates the E_t flow between the jets (the "underlying event") and produces events which are too coplanar. The E_t flow and $\Delta\phi$ distributions are completely insensitive to the choice of structure functions or the Q^2 scale.

For the results shown, direct, resolved, and VDM processes have been generated with the relative cross sections of 48%, 41% and 11% respectively, as determined from integrated parton-level cross sections for $\hat{p}_t$ greater than 2 GeV/c. After full detector simulation, triggering, and jetfinding, dijet events with average $p_t > 4$ GeV/c have relative contributions of 48%, 48% and 4% for direct, resolved and VDM processes respectively.

Different choices of proton structure functions or Q^2 scale change these relative contributions by not more than 5%, both for the input cross sections and in the final dijet sample. The relative contributions of the subprocess are somewhat more sensitive to the intrinsic transverse momentum (k_t) both in the proton and in the resolved photon. Both TWISTER and LUCIFER assume for the proton a Gaussian k_t distribution in each component with a width of 0.44 GeV. TWISTER assumes the standard first-order Altarelli-Parisi splitting distribution for the resolved photon ($\frac{dk_t^2}{k_t^2}$) with a lower limit of 0.5 GeV/c. One has some freedom in the Monte Carlo simulation to (for example) increase k_t in the proton and simultaneously reduce k_t in the resolved photon, maintaining agreement with the E_t flow and $\Delta\phi_{jj}$ distributions. Within reasonable limits such changes result in ranges of 48% to 60%, 33% to 48%, and 4% to 9% for direct, resolved, and VDM processes respectively. One can also fit the shapes of $\Delta\phi_{jj}$ and other distributions to estimate the relative contributions of resolved and direct processes. Using the default k_t values in TWISTER and LUCIFER, fits to six distributions gives a direct contribution which ranges from 40% to 55%, in reasonable agreement with the result above. We conclude that, with reasonable variations of relevant parameters, our data are consistent with a direct photon contribution of 40% to 60%, a few percent contribution from VDM processes, and the remainder from resolved photon processes.

LUCIFER also models "low p_t" physics by treating the photon as a vector meson which undergoes soft interactions via the LUND low p_t model [17]. Out of 0.5 million low p_t events generated, only four passed a dijet cut with average p_t ¿ 3 GeV/c, and none passed a cut of 4 GeV/c. Assuming a total γp hadronic cross section of 100 microbarns, we conclude that less than 1% of our dijet events with $p_t > 3$ GeV/c could be fluctuations of low p_t interactions, and this fraction would be even less for our standard p_t cut of 4 GeV/c.

Now we turn to consideration of the spectator jet system. In the simple Born-level

picture, the direct-coupled photon is completely absorbed in the hard scattering process, producing no spectator jet. However in either VDM or resolved photon processes, a spectator system from the photon is expected. Therefore, a naive expectation is that direct coupling processes should have little or no energy in the photon direction, while resolved or VDM processes should produce substantial forward energy. It is therefore interesting to look at the forward energy flow into the beam calorimeter. Electromagnetic energy in the BCAL is subject to effects from pileup from nearby RF buckets as well as multiple soft photons accompanying the high energy photon which initiated the interaction. To avoid these problems, we estimate the hadronic energy in the beam calorimeter, based on the pattern of longitudinal energy deposition. We define the beam calorimeter hadronic energy to be the sum of the energies in the back three layers, with a slight correction to layer-two energy for spillover of electromagnetic energy from layer one. This algorithm underestimates the hadronic energy slightly, but it is insensitive to beam pileup or multiple soft photons. Data and Monte Carlo have been treated identically.

Figure 3 shows the beam calorimeter hadronic energy divided by the incident photon energy for dijet events with average p_t of 4 GeV/c or more. The most prominent feature of the data is a sharp peak at small values of forward energy which contains more than half of the events. In addition, there is a tail which extends to 0.3. The Monte Carlo curve reproduces the data reasonably well. Figure 3 also shows the Monte Carlo expectations for the contributions from the three subprocess to the forward energy flow. All three components exhibit the peaking at small forward energy with a tail extending out to higher energy. Contrary to naive expectations, the distributions for the resolved and direct processes are quite similar in the region below 0.15.

The pion data are an important tool to further explore the question of forward energy flow, since πp interactions have no direct component, except possibly for a small higher twist contribution [18]. Figure 4 compares the BCAL hadronic energy for pion and

photon data. In order to match the energy range for the pion data, only beam energies from 200-300 GeV have been used in this plot. Also, due to the poorer statistics for the pion data, the average p_t cut for dijet events is 3.8 GeV/c rather than 4 GeV/c. Neither of these differences has a significant effect on the distributions. The forward energy distributions for the pion and photon data are surprisingly similar; in particular the pion distribution is also dominated by a peak at small BCAL energy. The forward energy decreases with an increasing p_t cut, as expected from energy conservation, but the similarity of the forward energy for γp and πp events is independent of p_t. However, pion and photon data do show substantial differences in many other distributions, such as E_t flow, E_t not associated with either jet, and $\Delta\phi_{jj}$. [19].

We conclude that there is not a clear separation of events into "direct" and "resolved" categories based only on forward energy flow. Contrary to naive expectations, Monte Carlo simulations indicate that direct and resolved processes have similar forward energy distributions. This conclusion is supported by the similarity of forward energy distributions for jets produced in πp and γp interactions. Within the context of the Monte Carlo simulations, the similarity arises because the resolved photon events, which have a forward-going beam jet, often deposit little or no energy in the forward direction, due to fluctuations in the beam jet fragmentation, and the direct-coupled events occasionally produce significant energy in the forward calorimeter due to fluctuations in the fragmentation of the high p_t partons. We conclude that a clean separation of direct coupling from the other subprocesses will require additional information, such as angular correlations and energy conservation constraints.

In summary, we have observed dijet production in γp interactions. The E_t flow and $\Delta\phi_{jj}$ distributions show clear evidence for jet production, in agreement with expectations from QCD. The data are in good agreement with a QCD Monte Carlo simulation which has approximately equal contributions from direct coupling and resolved photon processes,

with a few percent contribution from VDM processes. A somewhat surprising result is that the forward energy flow is very similar for pion-induced and photon-induced dijet events. However, within the context of the Monte Carlo simulation, this similarity is expected, since the forward energy flow is similar in the direct and resolved processes.

We wish to thank all those personnel, both at Fermilab and at the participating institutions, who have contributed to this experiment. We would especially like to thank Larry Cormell for contributions in the early phases of the experiment and Dave Northacker for excellent technical contributions. The authors would like to thank Tom Fields and Hugh Montgomery for useful discussions. This work was supported in part by the Particle Physics and Nuclear Physics divisions of the National Science Foundation, and the Nuclear Physics and High Energy Physics Divisions of the U. S. Department of Energy.

References

[1] See, for example F. Abe et al., Phys. Rev. Lett. **68**, 1104 (1992); C. Albajar et al., Phys. Lett. **B263**, 551 (1991); G. Arnison et al., Phys. Lett. **B172**, 461 (1986); M. W. Arenton et al., Phys. Rev. Lett. **53**,1988 (1984).

[2] M. R. Adams et al., Phys. Rev. Lett.**69**, 1026 (1992) ; M. Arneodo et al., Z. Phys. **C36**, 527(1987).

[3] See, for example B. Adeva et al., Phys. Lett.**B263**, 551 (1991); W. Braunschweig et al., Z. Phys. **C47**, 187 (1990);S. Komamiya, Phys. Rev. Lett. **64**, 987 (1990) D. Bender et al., Phys. Rev. **D31**, 1 (1985).

[4] R. Barate et al., Phys. Lett. **B174**, 458 (1986); E. Auge et al., Phys. Lett. **B168**, 163 (1986);P. Astbury et al., Phys. Lett. **B152**, 419 (1985); R. J. Apsimon et al., Z. Phys. **C46**, 35 (1990).

[5] M. Derrick et al., Phys. Lett. **B297**, 465 (1992); T. Ahmed et al., Phys. Lett. **B297**, 205 (1992).

[6] T. H. Bauer et al., Rev. Mod. Phys. **50**, 261 (1978).

[7] G. A. Schuler and T. Sjostrand, CERN-TH-6796-93; G. A. Schuler and T. Sjostrand, CERN-TH.6718/92.

[8] H. Baer, J. Ohnemus, J. F. Owens, Phys. Rev. **D40**, 2844 (1989); J. F. Owens, Phys. Rev. **D21**, 54 (1980).

[9] M. W. Arenton et al., Phys. Rev. **D31**, 984 (1985); K. A. Johns, "The Calibration, Response, and Energy Resolution of a Segmented, Sampling Hadron Calorimeter between 10 and 130 GeV/c", Masters Thesis, Rice University, 1983, unpublished.

[10] John E. Huth et al., FERMILAB-Conf-90/219-E.

[11] M. D. Corcoran et al., Phys. Lett. **B259**, 209 (1991).

[12] D. W. Duke and J. F. Owens, Phys. Rev. **D26**, 1600 (1982).

[13] H. U. Bengtsson, G. Ingelman, Comput. Phys. Commun. **34**.251 (1985); G. Ingelman, Comput. Phys. Commun. **46**, 217 (1987); G. Ingelman and A. Weigend, Comput. Phys. Commun. **46**, 241 (1987).

[14] F. E. Eichten, I. Hinchliffe, K. Lane, C. Quigg, Rev. Mod. Phys., **56**, 579, (1984).

[15] R. D. Field and R. P. Feynman, Nucl. Phys. **B136**, 1 (1978).

[16] B. Andersson, G. Gustafson, G. Ingelman, T. Sjostrand, Phys. Rep. **97**.31 (1983); T. Sjostrand, Comput. Phys. Commun. **39**, 347(1986).

[17] B. Andersson, G. Gustafson, I. Holgersson, O. Manson, Nucl. Phys. **B178**, 242 (1981).

[18] C. Naudet et al., Phys. Rev. Lett. **56**, 808 (1986).

[19] D. Naples, "The A-Dependence of $K_{t\phi}$ of Photoproduced Jets", in the Proceedings of the Fermilab Meeting of the American Physical Society Division of Particles and Fields, C. Albright, P. Kasper, R. Raja, and J. Yoh editors, World Scientic, p. 948 (1993).

Figure captions

Figure 1. Experimental apparatus. C1, C2, B1 and B2 are beam scintillators, PWC's are proportional wire chambers, DC's are drift chambers.

Figure 2. (a) E_t flow per event for dijet events with average jet p_t greater than 4 GeV/c. The higher p_t jet defines $\phi = 0$, and each calorimeter tower is plotted at the appropriate ϕ, weighted by the tower E_t. The points are data; the dashed line is Monte Carlo using independent fragmentation, and the solid line is Monte Carlo using string fragmentation. (b) $\Delta\phi$ between the jets for dijet events with average p_t greater than 4 GeV/c. Notation

is the same as in (a). The Monte Carlo curve is normalized to the same number of dijet events as the data.

Figure 3. Hadronic energy in the beam calorimeter divided by the photon energy, for dijet events with average p_t greater than 4 GeV/c. The diamonds are data, the curves are Monte Carlo. The solid histogram is all processes, normalized to the same number of events as the data. The dotted histogram is the direct coupling contribution, the dashed is the resolved photon, and the dot-dash line is the VDM contribution.

Figure 4. Hadronic energy in the beam calorimeter divided by the beam energy, for dijet events with average p_t greater than 3.8 GeV. The solid diamonds show γ-proton events, and the open squares show π-proton events. The π-p curve is normalized to the photon data.

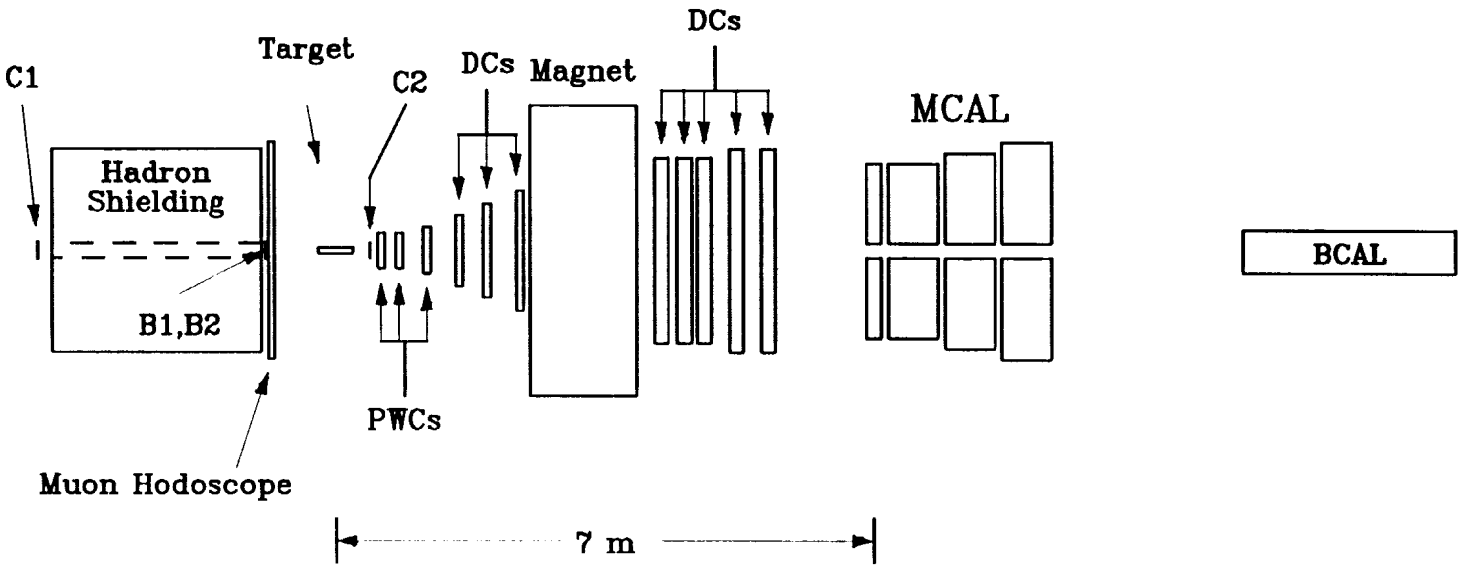
C1
Target
C2
DCs
Magnet
DCs
MCAL
Hadron
Shielding
B1,B2
PWCs
Muon Hodoscope
7 m
BCAL

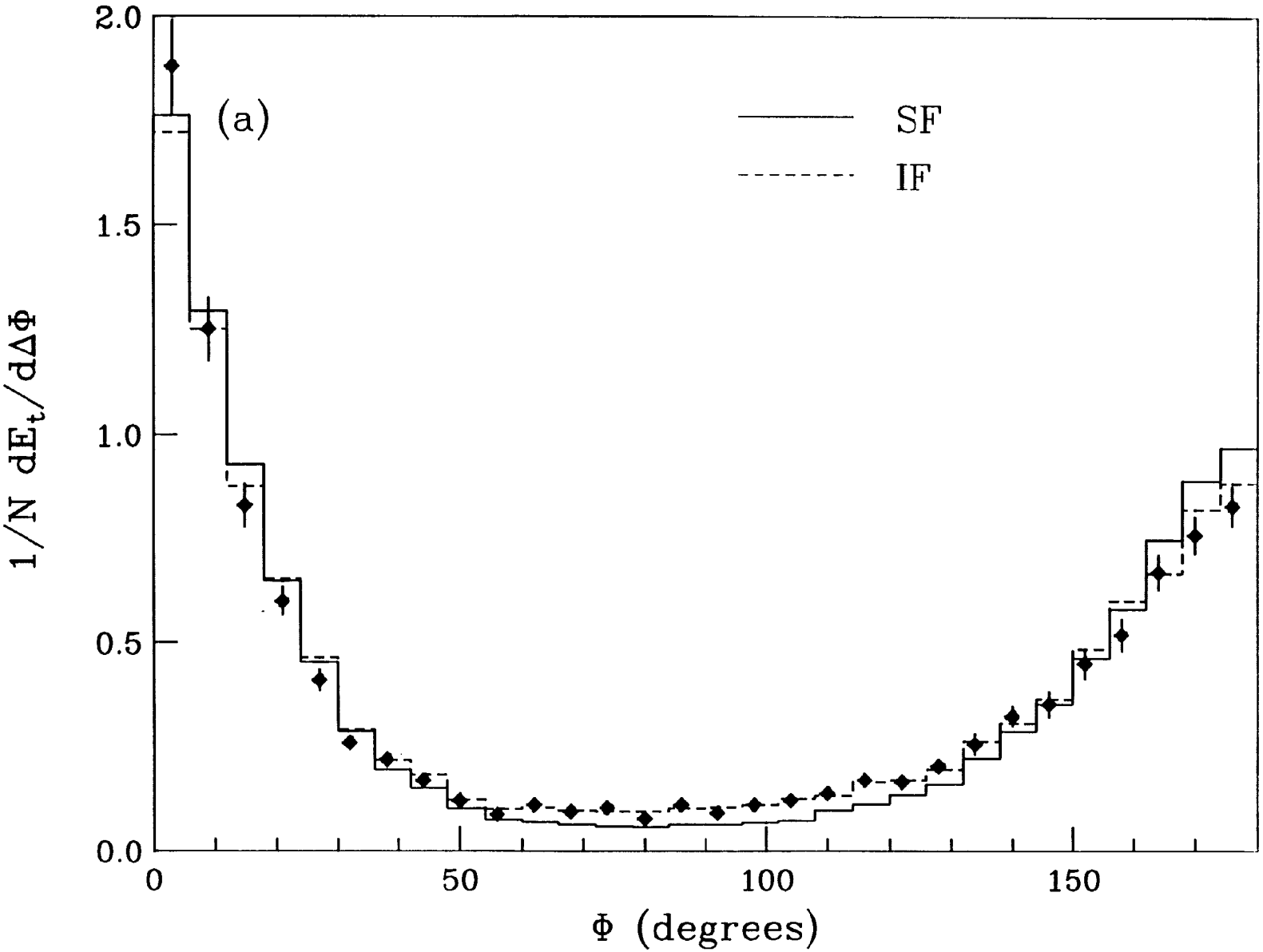

Figure 2(a)

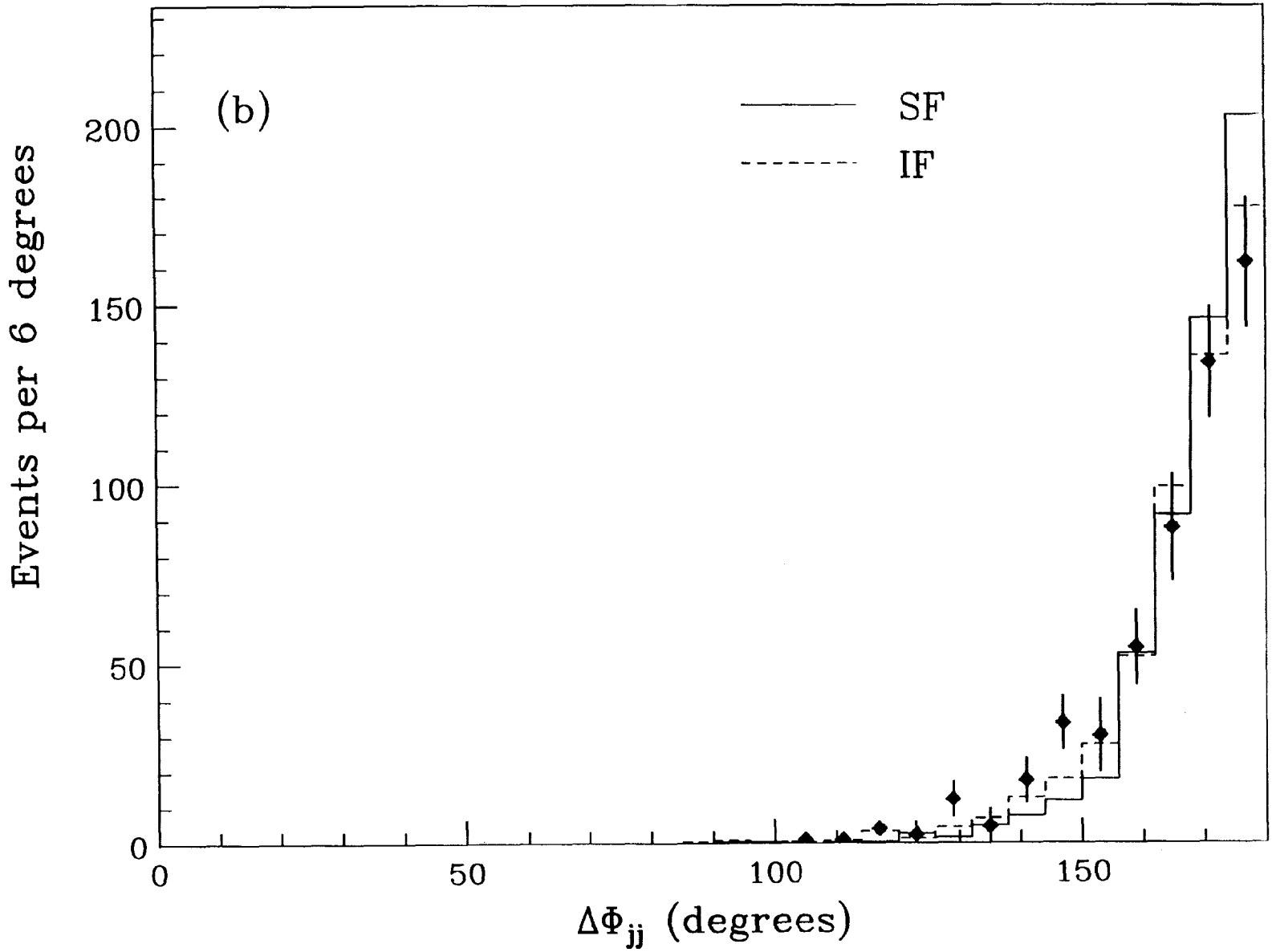
(b)
SF
IF
Events per 6 degrees
200
150
100
50
0
0
50
100
150
$\Delta\Phi_{jj}$ (degrees)

Figure 2(b)

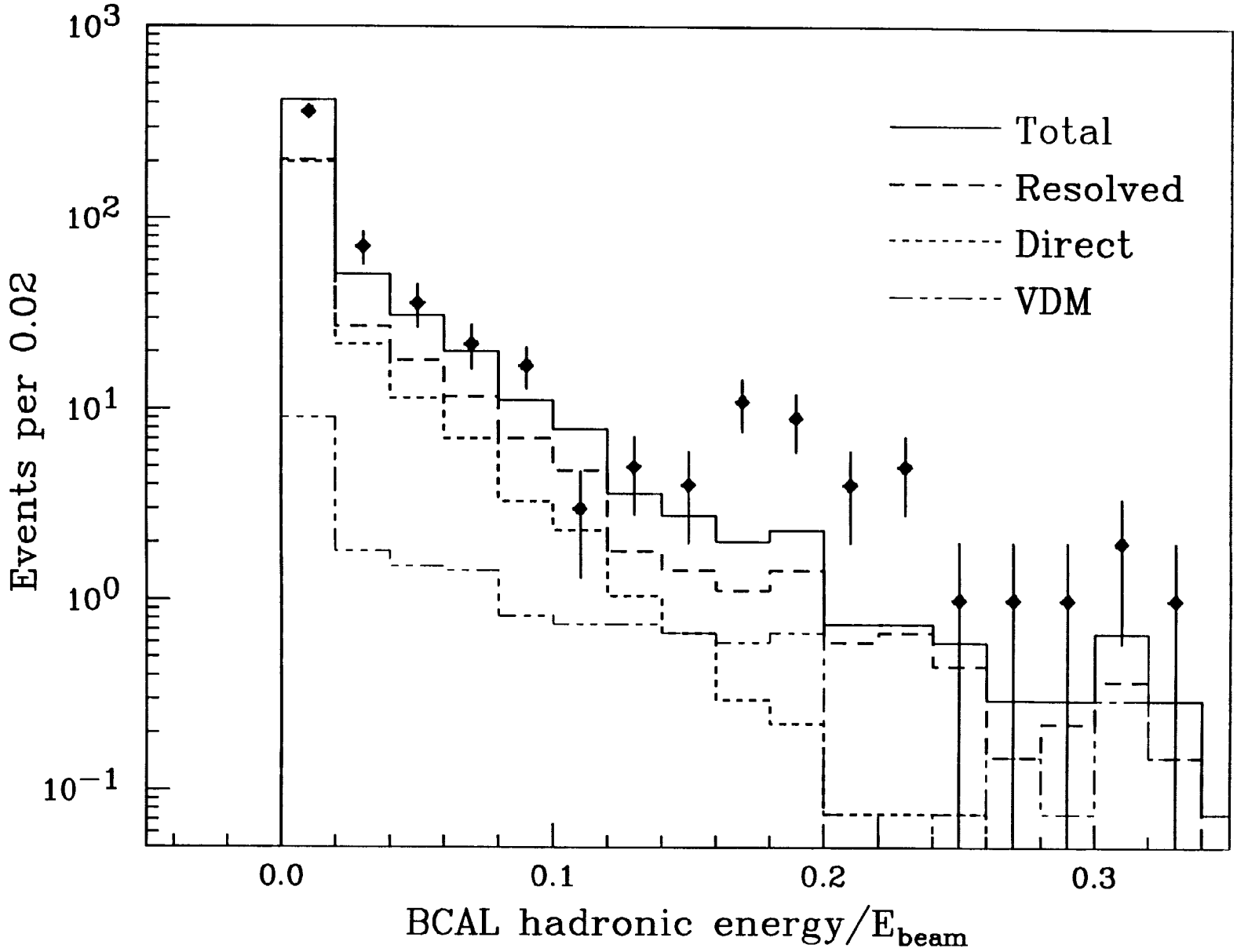
Total
Resolved
Direct
VDM
Events per 0.02
10^3
10^2
10^1
10^0
10^{-1}
0.0
0.1
0.2
0.3
BCAL hadronic energy/E_{beam}

Figure 3

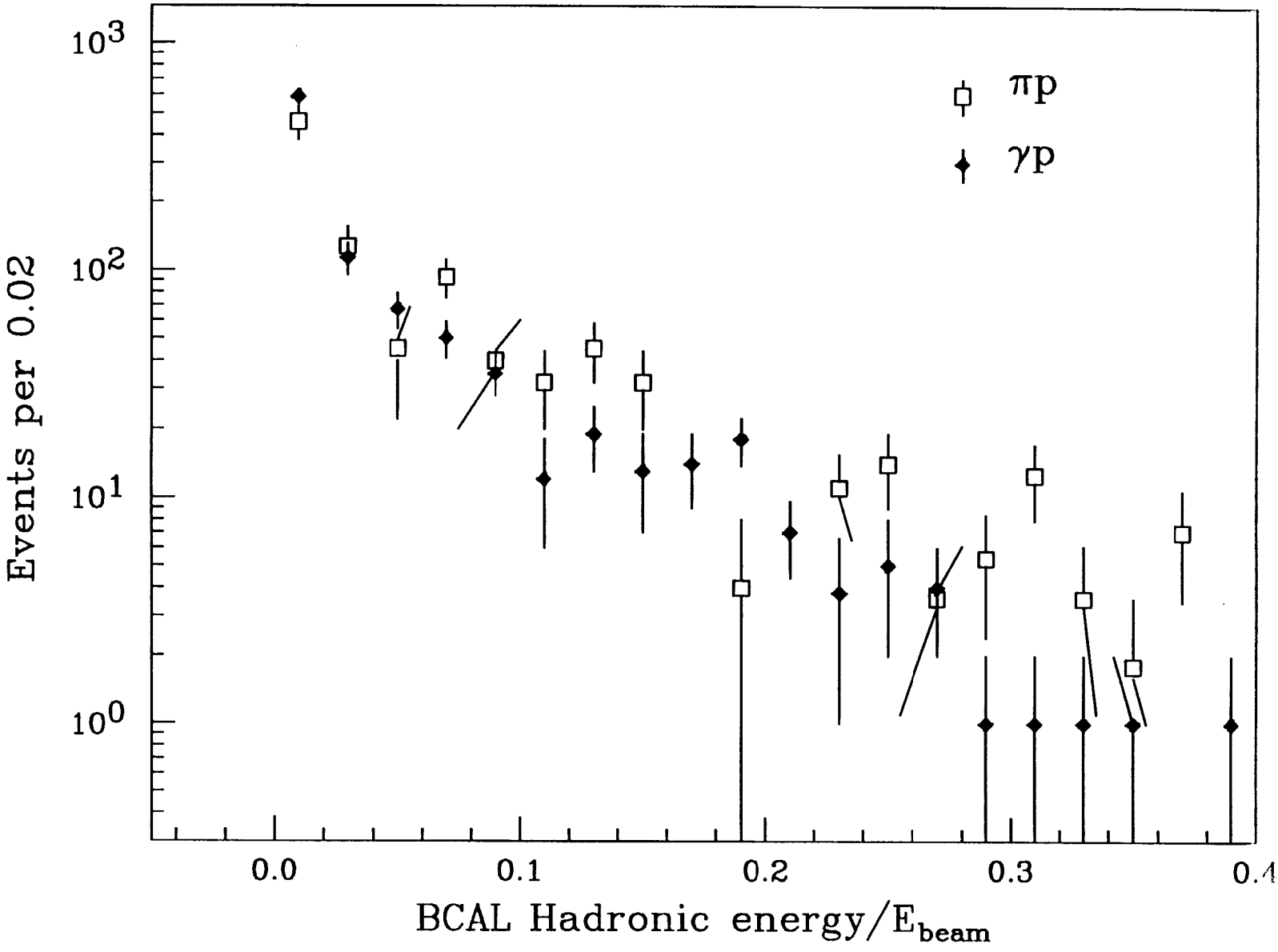
πp
γp
Events per 0.02
10^3
10^2
10^1
10^0
0.0
0.1
0.2
0.3
0.4
BCAL Hadronic energy/E_{beam}

Figure 4